Development of jacket substructure systems supporting 3MW offshore wind turbine for deep water sites in South Korea

Thanh-Tuan Tran [a, b], Daeyong Lee [a, *]

[a] Institute of Offshore Wind Energy, Kunsan National University, Jeollabuk-do, Republic of Korea
[b] Faculty of Engineering and Technology, Quy Nhon University, Binh Dinh, Viet Nam

ARTICLE INFO

ABSTRACT

This study aims to develop jacket substructures supporting a 3MW Offshore Wind Turbine (OWT) in water depth ranges of 25–40 m. A simplified structural design process is introduced and influences of jacket topological forms and brace systems on their dynamic performances are assessed. The results conclude that the topological configuration of the jacket substructure has a significant influence on the dynamic characteristics of the whole system, indicating a high priority when designing a jacket substructure for OWTs. Furthermore, two jacket substructures having the lowest material costs and the best performances under the Korean ocean environmental conditions are suggested. Additionally investigated in this study is a sensitivity of environmental loading directions on the structural performances of the jacket substructures. All the findings in this study might be very useful to assist the structural engineers when they design the support structures for large-scaled OWTs in the near future in South Korea.

1. Introduction

In recent years, Korea has been increasing embracing renewable forms of energy. According to the "Renewable Energy 3020" plan (Kim et al., 2020), the government will focus attention on solar and wind energy, with the ambitious goal of generating about 16.5 GW using wind power by 2030. With regards to this energy, the future lies in developing offshore wind farms to take advantage of higher offshore wind speeds and less turbulent airflow.

At present, South Korea has more than 90 Offshore Wind Farm Projects (OWFPs). Among them, five OWFPs are currently operating, and the other projects have been confirmed or are in the planning stage (4C Offshore, 2021). As known, almost all of the current Offshore Wind Turbines (OWTs) are deployed in the transitional water depth. Thus, in order to meet the rising energy demands, it is necessary to develop OWFPs in deeper waters for the upcoming projects (Oh et al., 2018; Shi et al., 2015). As stated by Refs. (EEA, 2009; Kang et al., 2011; Oh et al., 2018), increasing water depth leads to increasing overall costs of the offshore project. The cost of an offshore structure at a specific site, which is a function of the water depth and distance from the shore, can be calculated through the adjustment factors. For example, the total costs for foundations at water depths ranging from 40 to 50 m are 1.32 and 1.13 times greater than the cost for water depths of 20–30 m and 30–40 m, respectively (Kang et al., 2011). Thus, a suitable substructure plays a significant role since it can reduce the total cost of wind projects efficiently.

Currently, various substructures (i.e., monopile, suction caisson, tripod, or jacket) are widely installed in offshore wind farms worldwide (Kim et al., 2014, 2016; Kim and Lee, 2015; Sandal et al., 2018; Tran et al., 2020). A typical monopile comprises a steel tube pile that is popularly installed in shallow waters. In contrast, the jacket and tripod systems are mainly deployed for use in deeper water (Kim et al., 2016; Tran et al., 2020, 2022). The tripod system is composed of three steel piles arranged in an equilateral triangle, while the jacket substructures are assembled from steel tubular members comprised of a space frame structure (Wu et al., 2019). For the Korean environmental conditions, the jacket substructures are recommended considering their feasibilities and availability of installing equipment (Kim and Lee, 2015; Shi et al., 2013a, 2013b; Tran et al., 2022). Consequently, the current work only studies the jacket substructures.

This study focuses on the development of jacket substructures supporting an existing 3 MW wind turbine at different water depths (i.e., 25 m, and 40 m) under Korean environmental

conditions. The jacket substructures are designed based on the main design requirements. First, the dynamic characteristics of the whole system are evaluated to fix the target frequencies, followed by strength check under the possible situations according to codes (DNV-OS-J101, 2014; DNVGL-ST-0126, 2018; IEC 61400-1, 2005; IEC 61400-3, 2009). Moreover, the material consumption is also compared to select the most cost-effective design. A significant factor here is that the reasonable jacket substructure for each water depth will be selected through a feasibility analysis. The objectives of this study are summarized as follows:

- Providing the design procedure to develop jacket substructures supporting offshore wind turbines
- Proposing reasonable jacket substructures for upcoming offshore wind farms in South Korea
- Identifying the critical response-critical directions of jacket substructures when being installed

2. Description of reference wind turbine

The reference wind turbine used in this study is adopted from the POSCO (2017). The main characteristics of the turbine are shown in Fig. 1. It is a three-bladed upwind design with 3 MW rated power. The rotor consists of the blades and hub with a total mass of 64.6 ton. The nacelle houses the gearbox, generator, shaft, brake disc, etc., having a mass of 128.0 ton. These components are connected together, forming the Rotor-Nacelle-Assembly (RNA). The tower is in a steel tubular shape with a height of 56.77 m, providing support to the RNA. The diameters of the tower are assumed to vary

linearly between 4.5 m (bottom) to 3.07 m (top), and their corresponding thicknesses vary linearly from 34 mm (bottom) to 18 mm (top), respectively.

3. Design process for jacket substructures

The simplified design procedure for the OWT jacket substructure is introduced in this section. The input data (i.e., turbine geometries, site-specific environmental data, and geotechnical data) for the design process have been collected from the specific project (POSCO, 2017). The initial configurations (i.e., jacket height, leg spacing, jacket slope, and number of jacket layers) are selected. The jacket modeling is then completed with the main design requirements in terms of natural frequency and structural integrity (DNVGL-ST-0126, 2018; IEC 61400-1, 2005). The design process for the jacket substructure includes the three main steps, which is depicted in Fig. 2. The process is considered to be complete when the structural integrity satisfies the design requirements (DNVGL-ST-0126, 2018; IEC 61400-1, 2005).

3.1. Step 1: selecting initial jacket dimensions

The main parameters of the jacket are depicted in Fig. 3 and the relevant formula are summarized in Fig. 4. It is assumed that the jacket substructure does not have to be limited to a particular number of legs or bays. These parameters are derived as follows:

- Jacket height (h_J) is defined as the distance from the seabed to the bottom of the transition piece (TP). This parameter is chosen
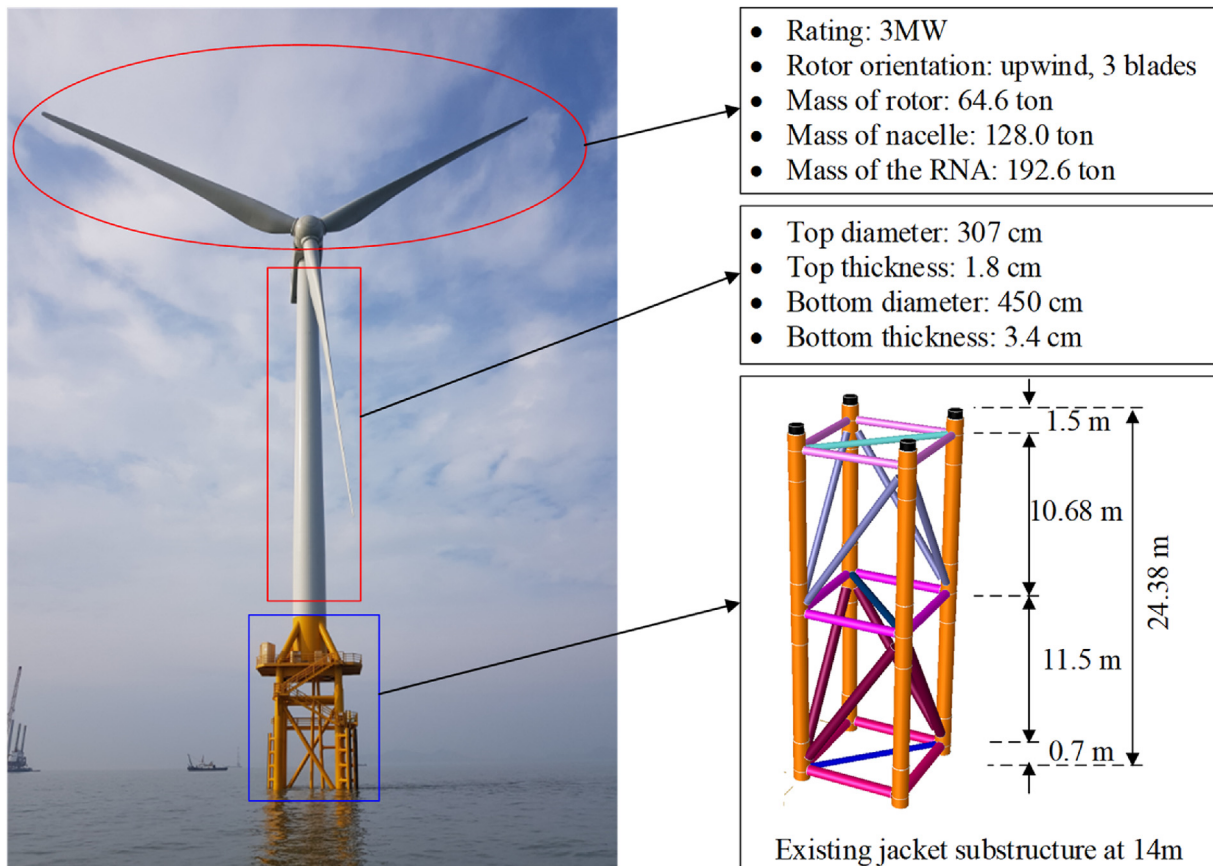

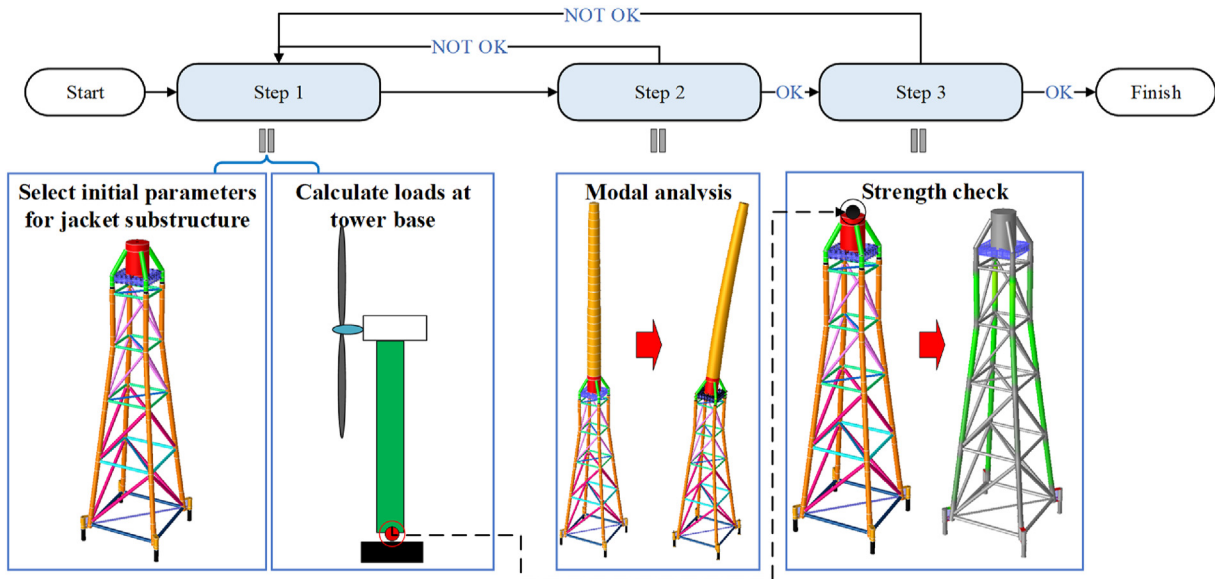**Fig. 1.** Reference 3 MW OWT (POSCO, 2017).

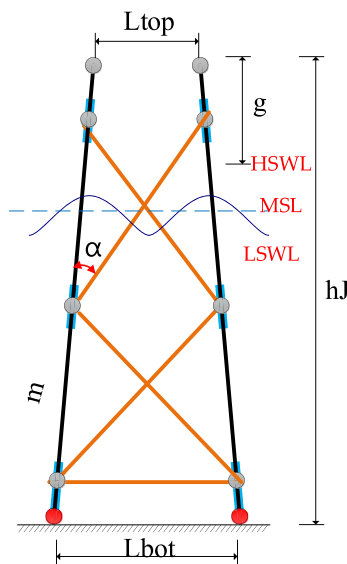**Fig. 2.** Design process for a jacket substructure.

Fig. 3. Main parameters of jacket substructure.

such that there is no effect of the splash zone on the transition piece. And h_J is calculated as follows:

$$h_J = HSWL + g \tag{1}$$

where, $HSWL$ is the high still water level in the considered environmental conditions; and g is the air gap, which is at least 20% of the 50-year significant wave height $H_{m,50}$ and a minimum value of 1.0 m (DNVGL-ST-0126, 2018).

- The transition piece is a complex component, which aims to transfer loads from the turbine to the jacket. It is difficult to design and there is no general process for selecting the type of TP. Configuration of TP depends on the tower geometry, number of legs, DLCs, and the required spacing for the working platform, etc. In this research, the jacket substructures are designed to

support the existing 3 MW OWT; the configuration of TP is taken from the previous references (POSCO, 2017; Tran et al., 2022).
- The leg top spacing (L_{top}) is then determined from the configuration of the transition piece.
- Next, the initial slope (m) of the jacket substructure is defined. According to Refs. (El-Reedy, 2014; Jalbi and Bhattacharya, 2020), m varies from 1:6 to 1:10.
- Spacing of the leg bottom (L_{bottom}) is a function of h_J, L_{top}, and m parameters, and it is calculated using Eq. (2).

$$L_{bottom} = L_{top} + mh_J \tag{2}$$

- A number of jacket layers (n) are designed based on NORSOK-N004 (2004). It states that the angle between brace and leg should be in the range from 30 ° to 90 °.
- Finally, the bay lengths and heights of each layer are determined.

3.2. Step 2: natural frequency analysis

In this step, the support structure will be checked with the allowable frequency range (POSCO, 2017). This is important to avoid the resonance effects caused by the rotor or blade passing.

3.3. Step 3: extreme event analysis

This step aims to evaluate the structural integrity of the jacket substructure. The loads acting on the jacket substructures will be determined first, followed by static numerical analysis and strength check in accordance with standard designs (DNVGL-ST-0126, 2018; NORSOK, 2004).

3.3.1. Loading acting on the jacket substructures

3.3.1.1. Environmental loads (Env.)
In this study, the jacket substructures are designed based on environmental conditions in the Korean Southwest Sea. The wind and wave parameters are selected from metocean analysis
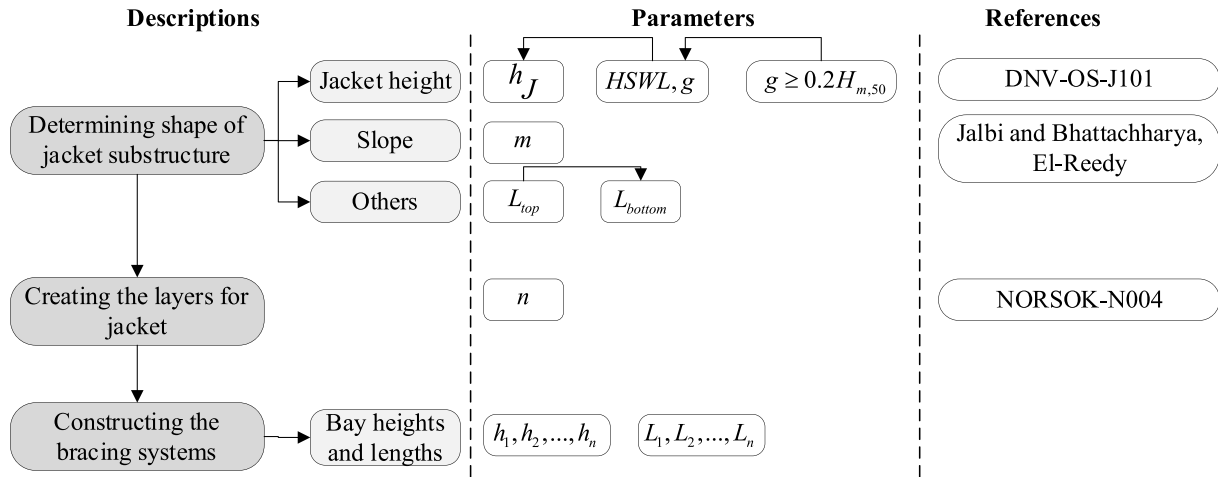
Fig. 4. Relevant formula for selecting jacket dimensions.

provided in POSCO (2017). The wind load of 50-year conditions is selected for evaluation of the extreme aerodynamic loads. The 10-min mean wind speed at the hub height (42.5 m/s) is selected for designing the substructure.

For the hydrodynamic effects, wave data is considered in terms of wave height, wave period, and wave direction. The significant wave height of the 50-year return period ($H_{s,50}$) is 5.97 m, which is taken from POSCO (2017). The corresponding zero-crossing period (T) are calculated as (DNVGL-ST-0126, 2018):

$$T_{min} = 11.1 \sqrt{\frac{H_{s,50}}{g}} \leq T \leq 14.3 \sqrt{\frac{H_{s,50}}{g}} = T_{max} \tag{3}$$

The 50-year maximum wave height is the function of 50-year significant wave height and can be calculated using Eq. (4):

$$H_{m,50} \approx 1.86 H_{s,50} \tag{4}$$

Moreover, the current load acting on the jacket substructure is also considered. The current loading model is assumed to be constant along the sea level with a speed of 1.04 m/s over the 50-year return period. The impact of marine growth is adopted with thickness ranging between 5 and 10 cm.

With regards to the loading directionality, different angles ranging from 0° to 360° at an interval of 15° are applied to the jacket substructure, as presented in Fig. 5. For the numerical analysis that processes the critical environmental loading conditions, the environmental loads (wind, wave, and current) acting on the jacket substructure are assumed to be coincident.

3.3.1.2. Design load cases (DLCs)

For the Ultimate Limit State (ULS) analysis, Design Load Cases (DLCs) at the tower base are usually generated from integrated time-domain simulations using GH-Bladed (Bossanyi, 2010). These
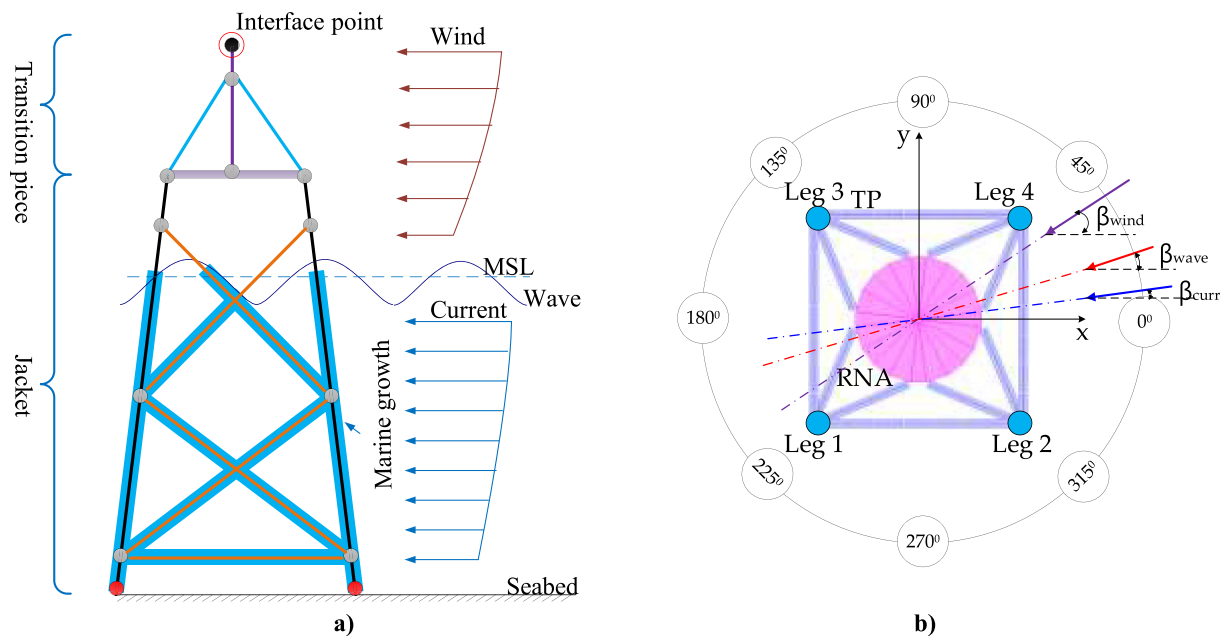

Fig. 5. Directionality of environmental loading.

load cases are established to cover all possible operation situations occurring throughout the lifetime of the system, and they are defined according to Refs. (Böker, 2010; DNV-OS-J101, 2014; DNVGL-ST-0126, 2018; IEC 61400-1, 2005; IEC 61400-3, 2009). The Design Load Cases considered for the ULS analysis in this study can be found in Tran et al. (2022).

3.3.2. Structural integrity

Static numerical analysis is performed under DLCs using SACS software (Bentley, 2019), and strength check will be done in accordance with c. In order to measure the strength capacity of the jacket members and joints, the Unity Check (*UC*) is utilized. The *UC* is defined as follows:

$$UC = \frac{\sigma_m}{\sigma_{Rd}} \qquad (5)$$

In which, σ_m and σ_{Rd} are the actual and allowable stresses. The *UC* formulations of the tubular member and joint can be found in section 6.3 and 6.4 of NORSOK (2004).

4. Modeling of jacket structures

4.1. General descriptions

Using the design process described in Section 3, the jacket substructures are built to support the existing 3 MW wind turbine. Different jacket configurations, categorized into two groups (i.e., 4LJ-25 and 4LJ-40) at different water depths (i.e., 25 m and 40 m) are developed (Fig. 6). The first group has a total height of 46 m, installed at a 25 m sea level (Fig. 6a). Three brace levels that comply with the criteria of a minimum angle of 30 ° between leg and brace are implemented. In the case of 40 m sea level, the jacket substructures have a total height of 61 m (Fig. 6b) and four brace levels.

For each sea level, this study considered various topological forms (i.e., $m = 0$ and $m = 10$) and bracing systems (i.e., Pratt and X-brace). The jacket substructures are developed with these four configurations (Fig. 6). Except for the topological form, all of the other properties (material, jacket height, height of each layer) are the same. The structural parameters of the developed models are summarized in Fig. 6.
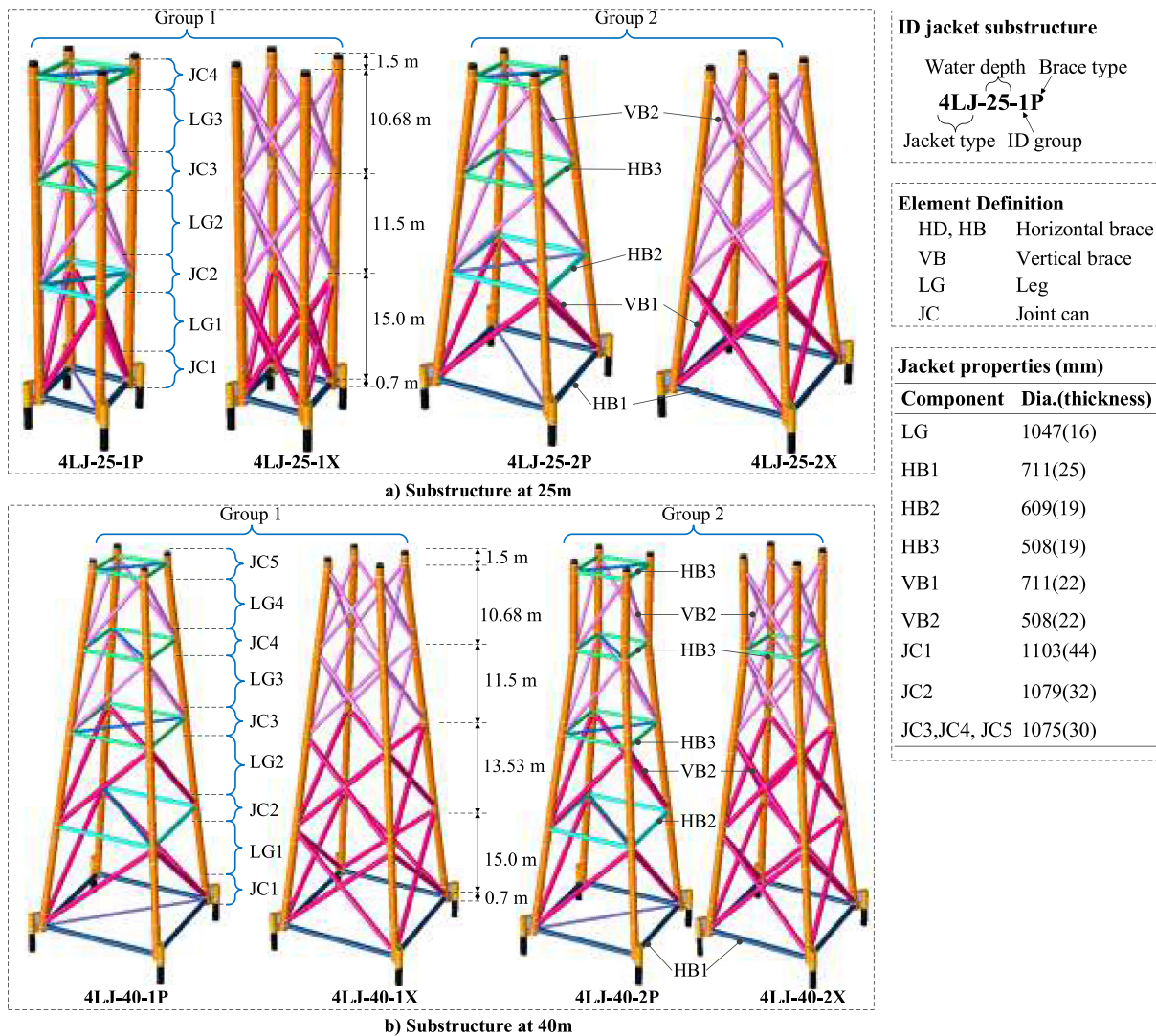

Fig. 6. Modeling of jacket substructure at different water depths.

4.2. Finite element model

The numerical modelings of the jacket support structures are developed using the software program SACS (Structural Analysis Computer System). The main components of the structure are the tower, transition piece, and jacket structure.

A detailed example of the jacket support structure (i.e., 4LJ-40-2P) is shown in Fig. 7. The Euler-Bernoulli beam elements are implemented to model the jacket substructure. The use of this element allows the linear behavior for axial, shear, torsion, and the cubic behavior for moment (Bentley, 2019). Cross-sections of the jacket legs and brace members are modeled as tubular sections with the corresponding parameters as shown in Fig. 6. The leg member is divided into three segments corresponding to its geometries, as depicted in Fig. 7d. The influences of the overlap and joint-can are also considered (Fig. 7e). The former is applied to avoid the duplication of brace members. The latter is simulated by increasing the size of the leg members at the intersection points. It is assumed that the jacket substructures considered in this study are installed using the pre-piling method; skirt pile connections at the jacket base are also considered in the analysis model (Fig. 7f).

In this research, structural properties of the tower and transition piece are the same as the existing jacket substructure installed at 14 m water depth, and their detailed geometry information can be found in Tran et al. (2021). The tower is composed of a combination of 22 elements, with a total height of 56.77 m. The Rotor Nacelle Assembly (RNA) is assumed as a lumped mass, and this is assigned at the tower top. In addition, four lumped masses are assigned along the tower, representing the masses of tower flanges, as depicted in Fig. 7a. Regarding the transition piece, shell elements are used for modeling the H-section beams, while the beam elements are used for modeling the tubular tube and support members (Fig. 7b). In this analysis, the access door in the cylinder will not be considered as using the beam element simulates the cylinder.

5. Feasibility analysis

This section aims to compare and evaluate the feasibility of jacket substructures developed for each sea level. In this regard, the numerical analysis will cover the main requirements given in Section 3.

5.1. Eigen analysis

Eigen analysis is first performed to compute the natural frequencies of the offshore wind turbine system. This is necessary to avoid the resonance phenomenon caused by the vibration of the rotor (1P) and blade-passing (3P). The 1P and 3P ranges are determined from the cut-in and rated rotor speed of the 3 MW OWT specification provided by Doosan Heavy Industry. In this study, the soft-stiff design, which is known as the most common design of the current support structures, is selected to optimize the economy. The comparative modal analyses of the jacket substructures are reported for the first four natural frequencies, as shown in Fig. 8.

5.1.1. Effects of the topological forms

As seen in Fig. 8, the topological forms have an important effect on the dynamic characteristics of the jacket. In Fig. 8a, corresponding to the sea level of 25 m, there is a significant difference between the two basic configurations (i.e., $m = 0$ and $m = 10$). Particularly, natural frequencies of the second topological form ($m = 10$) are found to be higher compared to those of the first topological form ($m = 0$). A maximum difference of 22.8% is found for the Pratt bracing system. This is due to the higher stiffness when considering the slope ($m \neq 0$), which is explained in Fig. 10. For the sea level of 40 m, there are slight changes in natural frequencies, with a maximum difference of up to 9.7%.
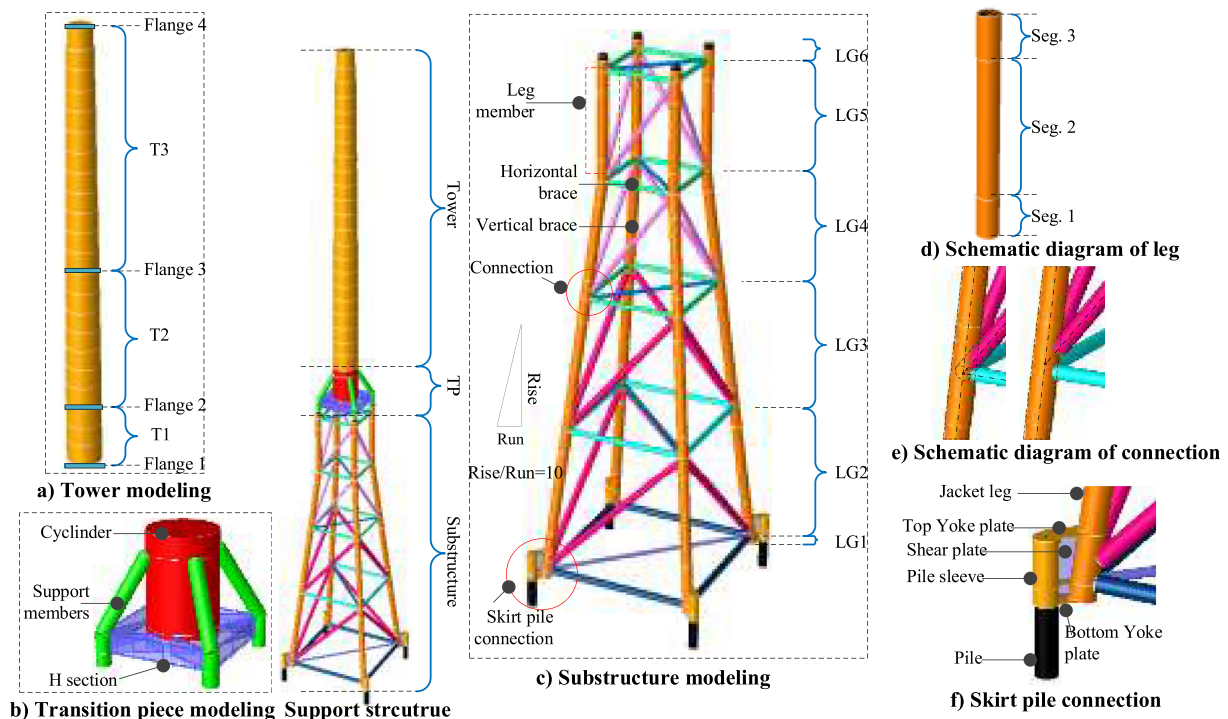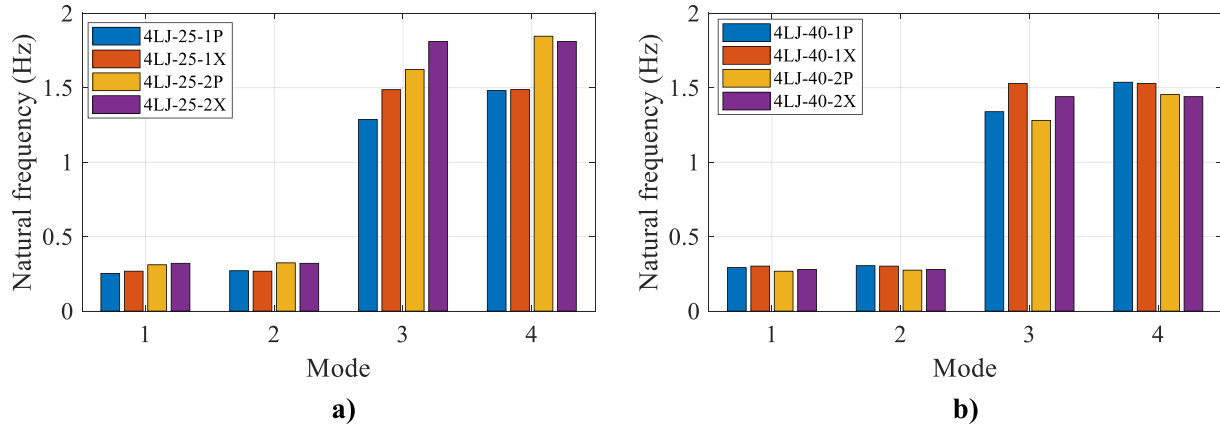

Fig. 7. Modeling of support structure.

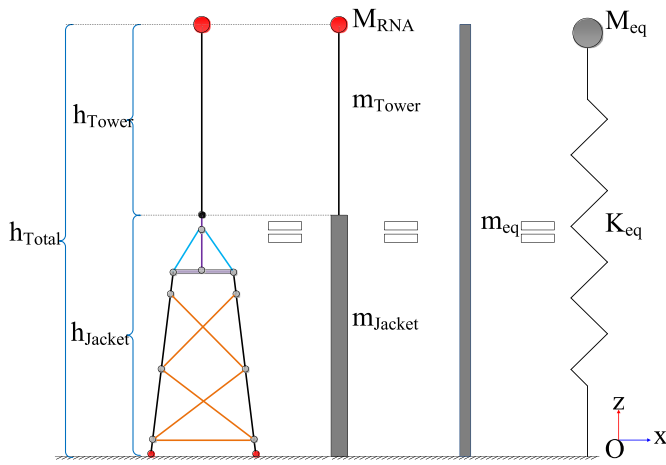**Fig. 8.** Comparison of natural frequencies: (a) 4LJ-25 and (b) 4LJ-40.

Fig. 9. Equivalent stiffness and mass of the support structure.

5.1.2. Effects of the bracing systems

Considering the bracing system, the X-type provides a higher stiffness than the Pratt type as expected. At the sea level of 25 m (Fig. 8a), the differences in natural frequencies between X- and Pratt braces are 6.0% and 3.1% for the first ($m = 0$) and second ($m = 10$) topological forms, respectively. At the higher water depth of 40 m (Fig. 8b), an average difference of 4% is found between X- and Pratt type braces.

The variations in the natural frequencies of the designed sub-structures can be explained based on the influences of their mass and stiffness. As stated by Jalbi and Bhattacharya (2018), the dominant frequencies (f_0) of the jacket system can be calculated as follows:

$$f_0 = \frac{1}{2\pi}\sqrt{\frac{K_{eq}}{M_{eq}}} \tag{6}$$

In which, K_{eq} and M_{eq} are equivalent stiffness and lumped mass of the system, respectively (Fig. 9).

The fundamental natural frequency (f_0) is taken from the numerical simulation and the equivalent lumped mass M_{eq} is given by Eq. (7).

$$M_{eq} = 0.243 m_{eq} h_{total} + M_{RNA} \tag{7}$$

In which, m_{eq} is the equivalent mass of the support structure, and it is taken from Jalbi and Bhattacharya (2018).

$$m_{eq} = \frac{m_{Jacket}\int_0^{h_{Jacket}}\varphi^2 dz + m_{Tower}\int_{h_{Jacket}}^{h_{Total}}\varphi^2 dz}{\int_{h_{Jacket}}^{h_{Total}}\varphi^2 dz} \tag{8}$$

The mode shape function φ is evaluated using the following equation:

$$\varphi = \beta\left(\sin\frac{\lambda}{L}z - \sinh\frac{\lambda}{L}z\right) + \cosh\frac{\lambda}{L}z - \cos\frac{\lambda}{L}z \tag{9}$$

where $\lambda = 1.8751$ and $\beta = -\frac{\cos\lambda + \cosh\lambda}{\sin\lambda + \sinh\lambda}$

Fig. 10 shows a comparison of the structural properties of different jacket configurations. At the sea level of 25 m (Fig. 10a), the second configuration provides a higher stiffness to the OWT, with an average difference of about 55.4%, while the difference of effective mass is about 5.6%. In the case of the deeper sea level (Fig. 10b), there are slight differences in effective stiffness and mass,
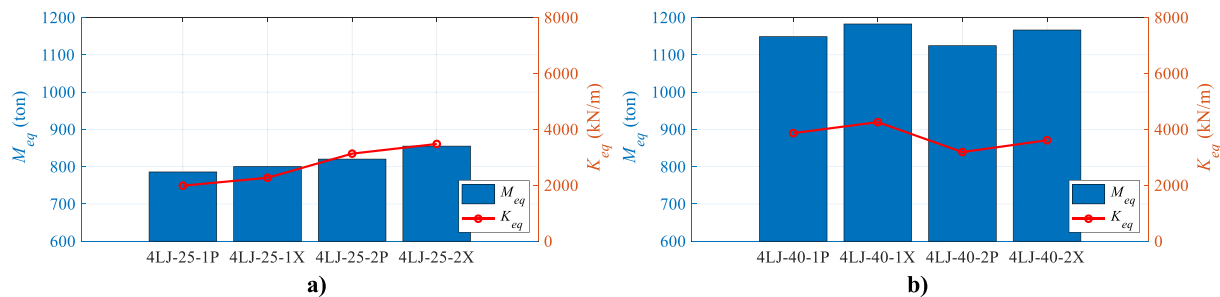

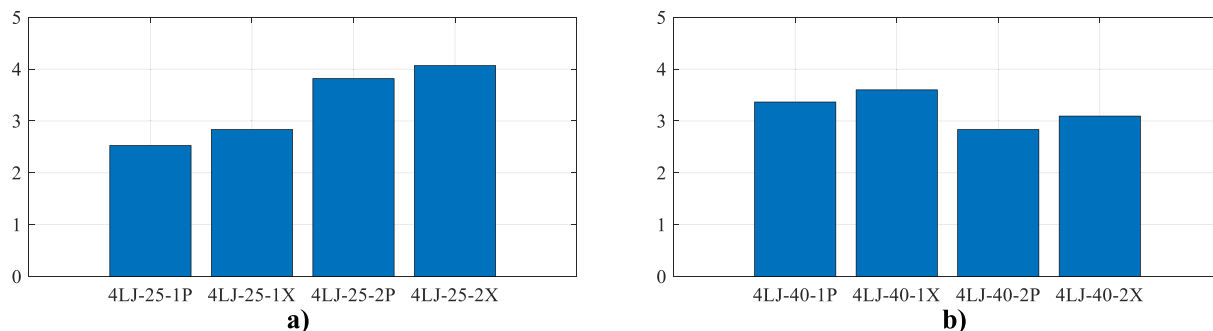**Fig. 10.** Structural properties of the support structures: (a) 4LJ-25 and (b) 4LJ-40.

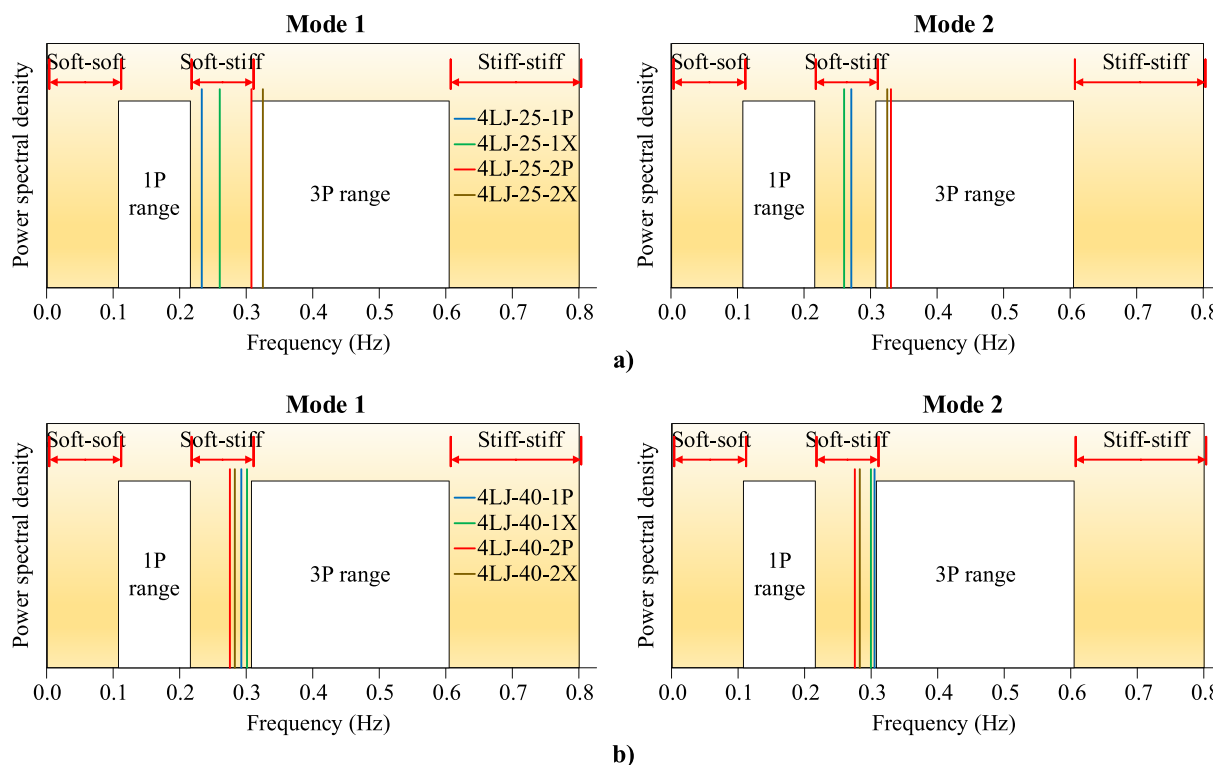**Fig. 11.** Stiffness-to-mass ratio: (a) 4LJ-25 and (b) 4LJ-40.

Fig. 12. Allowable frequency ranges: (a) 4LJ-25 and (b) 4LJ-40.

with values of 16.3% and 1.7%, respectively. The stiffness-to-mass ratios of all jacket substructures are presented in Fig. 11. As expected, a higher ratio correlates with a higher natural frequency. The ratio of X-brace is higher at 1.12 times compared to the Pratt brace in both cases.

5.1.3. Efficiencies of the jacket substructures

The efficiencies of the developed models are evaluated graphically in Fig. 12. As seen in Fig. 12a, the first topological form (4LJ-25-1) shows the soft-stiff design property, which is known to be the most common for the current offshore development. On the other hand, the dominant frequencies of the second topological form (4LJ-25-2) lie in the resonance area, which can lead to the structural resonance problem as well as fatigue damage.

Considering the deeper water (40 m) level, the natural frequencies of the designed structures lie in the soft-stiff range, and hence cross deployment does not lead to resonance (Fig. 12b). However, the second topological form (4LJ-40-2) shows smaller values compared to the first topological form (4LJ-40-1), with

average differences of 9% and 7% for the Pratt and X-bracing systems, respectively.

5.2. Ultimate limit state design

To evaluate the dynamic performance of jacket substructures under the ultimate limit state, jacket substructures are analyzed with twelve DLCs explained in Section 3.3. The maximum lateral displacement at the transition piece and the maximum stress of leg members are analyzed and compared. The maximum lateral displacements are the sum of displacement in X- and Y- directions and they are observed at the top of TP, whereas the maximum stresses are observed at the lower jacket legs. Comparisons of total displacement and stress response are presented in Fig. 13 and Fig. 14, respectively.

5.2.1. Effects of the topological forms

At the water depth of 25 m (Fig. 13a), there is a large difference between the two configurations considered (4LJ-25-1 and 4LJ-25-
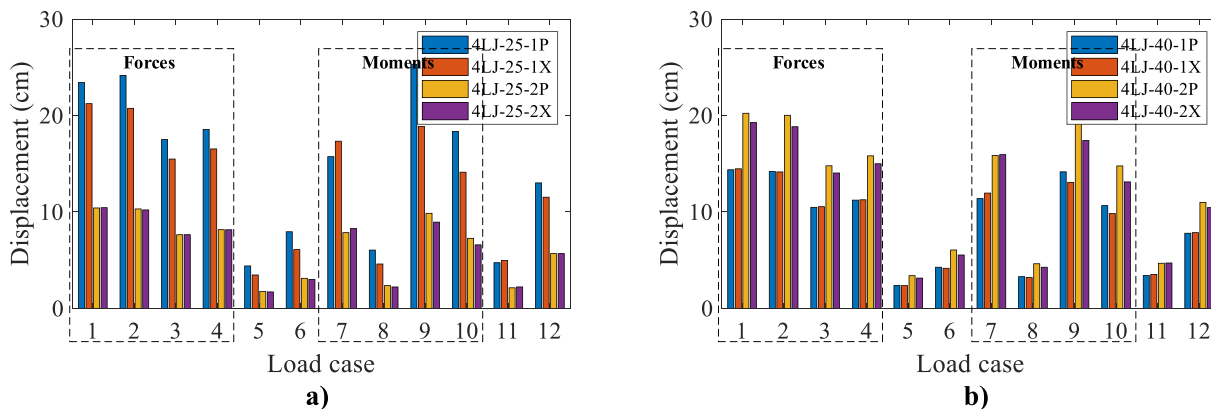
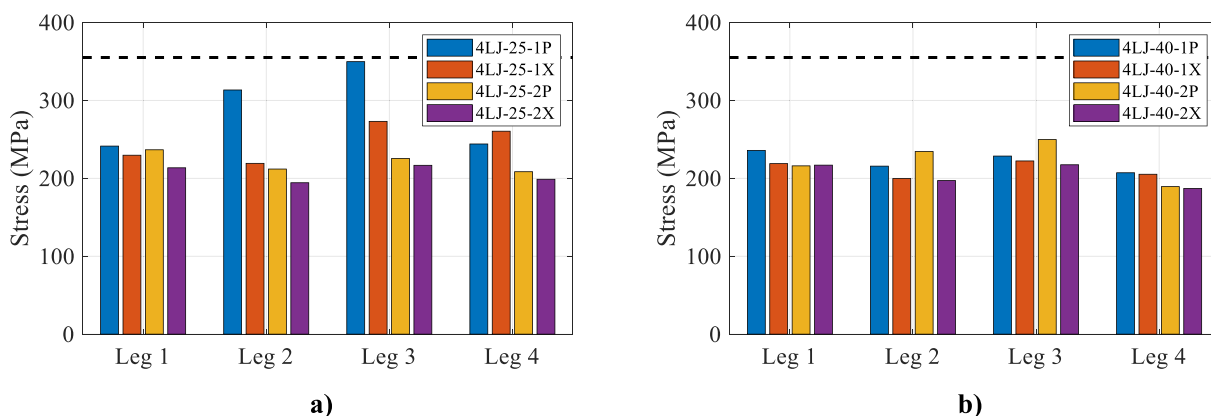**Fig. 13.** Histograms of total displacement: (a) 4LJ-25 and (b) 4LJ-40.

Fig. 14. Histograms of maximum stress: (a) 4LJ-25 and (b) 4LJ-40.

2). The larger response is found in the case of the first configuration; it is about 2 times compared to the second form. At the water depth of 40 m (Fig. 13b), the maximum response of the jackets is around 20 cm, and it belongs to the second configuration. Compared to the second configuration, the first form shows smaller differences, with an average difference of 50%.

Analysis of stress responses is performed to check the capacity of the selected jacket members. The results are shown in Fig. 14, where the dashed line is the yield strength of the material. In general, the leg members satisfy the strength criteria. At the sea level of 25 m, the first topological form reaches its ultimate strength earlier than the second form. However, in the case of 40 m, the stress distribution has a slight change. The stresses of each jacket leg member under twelve DLCs are graphically displayed in Appendix.

5.2.2. Effects of the bracing systems

According to Fig. 13, there are minor variations in lateral displacements between the bracing models. The largest differences are 16.1% and 4.7% at the sea water levels of 25 m and 40 m, respectively. In Fig. 13, the most significant finding from all models is that the response obtained from the X-brace system is smaller than that of the Pratt system. This is owing to the higher stiffness of X-bracing, which is explained in Section 5.1. Moreover, the structural response is primarily caused by the moments and forces in X- and Y- directions.

Under the ultimate design loads (Fig. 14), the flexural capacity of the X-type jacket substructure is higher than that of the Pratt brace type. Reduction values of 12% and 6.7% are found at the sea levels of

25 m and 40 m, respectively.

5.2.3. Design check

The strength checks for all jacket substructures are depicted in Fig. 15. All jacket members and joints are checked with NORSOK N-004 (2004). It shows that the *UC* factor is smaller than one, implying that the simulation results are within the safety zone.

5.3. Mass of jacket substructure

Fig. 16 presents a comparison of the masses of the jacket substructures for different sea levels. The results show that the average masses of the X-bracing system are about 10% higher than those of the Pratt system for both 4LJ-25 and 4LJ-40. At the water depth of 25 m (Fig. 16a), the mass of 4LJ-25-1P is 211 ton, showing a slightly smaller mass compared to 4LJ-25-1X (225 ton). Further, a difference of about 32 ton between Pratt and X-brace systems is found for the second configuration. At the deeper sea level 40 m (Fig. 16b), the jacket masses of all configurations are close to each other, with the X-bracing system heavier (around 30 ton) than the Pratt system. Since the transition piece and tower are the same, the trend of difference is the same for total weight of the support structure.

5.4. Selection of the optimal jacket substructure for wind turbine

Based on the outcomes, the following observations are drawn:

• At the water depth of 25 m (4LJ-25): The results from Eigen analysis indicate that the first group is in non-resonance
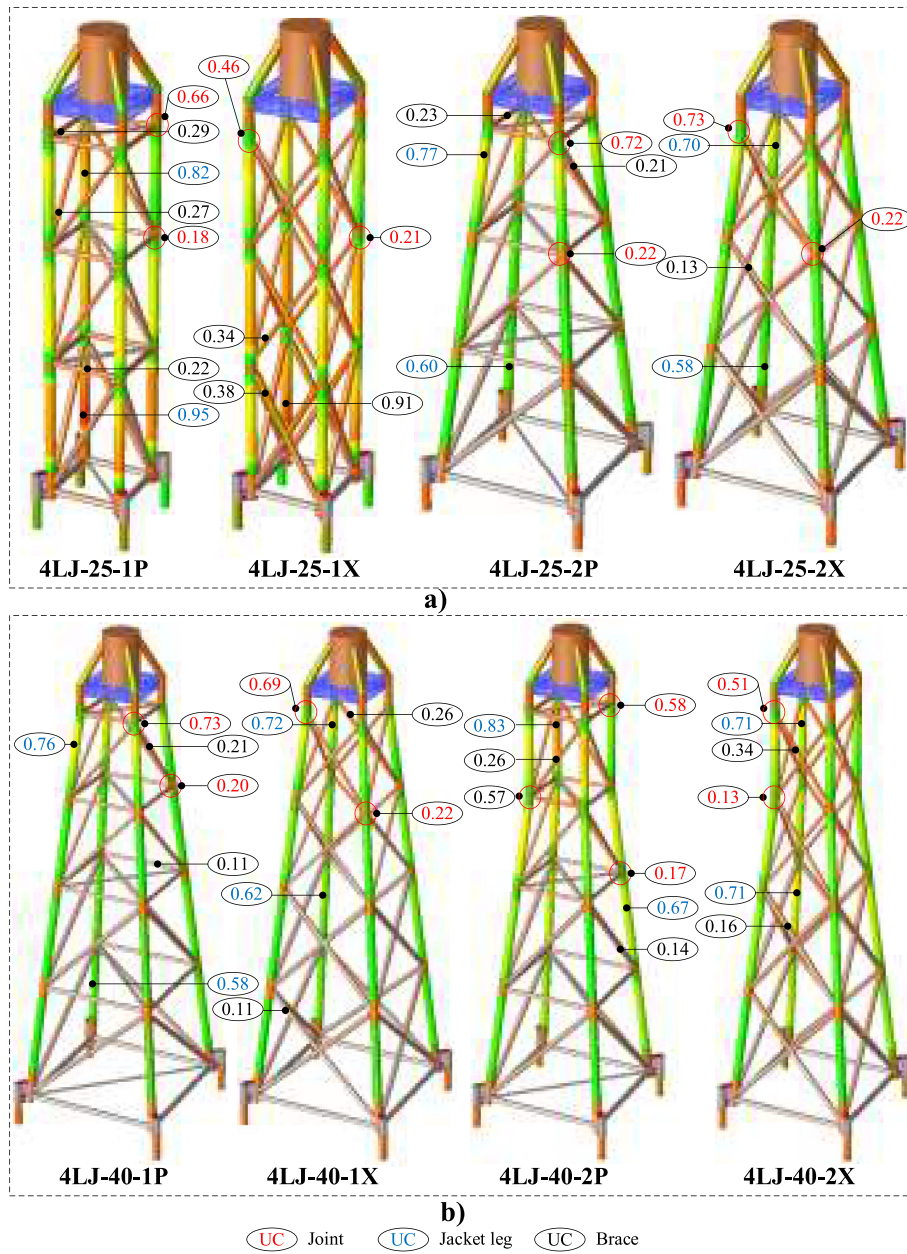
UC Joint   UC Jacket leg   UC Brace

Fig. 15. Results of strength check: (a) 4LJ-25 and (b) 4LJ-40.
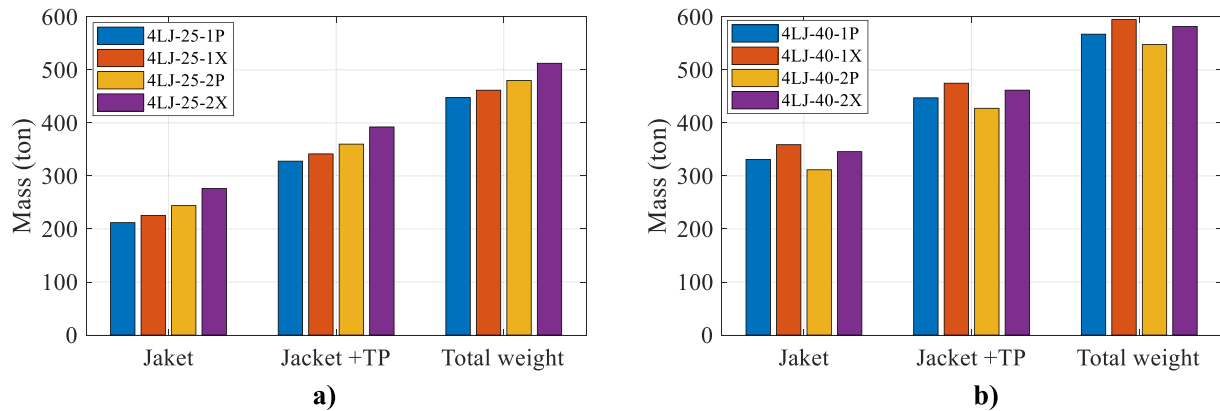

Fig. 16. Comparison of mass: (a) 4LJ-25 and (b) 4LJ-40.

structures, showing greater effectiveness compared with resonance substructures (second group). Under DLCs, all substructures satisfy the strength criteria; however, the Pratt brace form reaches its ultimate strength capacity earlier than the X-brace system. Thus, the first topological form with X-brace system (4LJ-25-1X) is selected as an optimal jacket substructure for a wind turbine at the water depth of 25 m (Fig. 17).

- At the water depth of 40 m (4LJ-40): Natural frequencies of all designed substructures are in the non-resonance area; notably, the first group is closer to the lower bound of the 3P range. Furthermore, these systems are within the safety zone. Relating to material costs, the second topological form with the Pratt brace system (4LJ-40-2P) is the most cost-effective substructure. Therefore, this concept is chosen as the optimal model for the sea level of 40 m (Fig. 17).

6. Critical directionality for installing jacket substructures

In the previous section, feasibility analyses were performed for all jacket substructures, aiming to select the reasonable jacket substructures for each sea level. In this section, the sensitivity of the selected jacket substructures to the environmental loading directionality is investigated. A schematic representation of loads acting on the jackets is provided in Fig. 18.

6.1. Structural performances under environmental loads (env)

Numerical simulations were conducted to find the critical bending direction of each jacket substructure. As described in Section 3.3.1, the environmental loading angles vary from $0°$ to $360°$ in steps of $15°$. The comparisons of lateral displacement at the TP are depicted by polar diagrams in Fig. 19. As can be seen, there is a distinct difference between the two basic configurations. At the water depth of 25 m (Fig. 19a), the total displacement of the jacket substructure (3.5 cm) is almost independent of the loading directions. Thus, their responses are visualized as a full circle in the polar diagram. For the deeper water (Fig. 19b), the critical displacements are found at the angles of $135°$ and $315°$, with a value of about 3.4 cm.

The comparative stresses of the jacket substructures are reported in Fig. 20. In general, the individual values vary with a
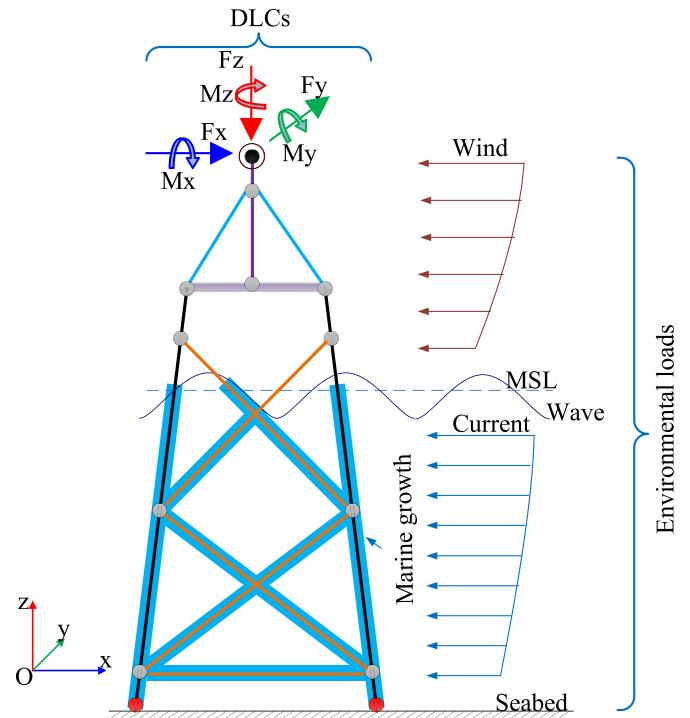

Fig. 18. Loads acting on the jacket substructures.

discernible trend to the loading orientation. At the water depth of 25 m (Fig. 20a), stress responses have the same trend for all jacket legs, with the maximum stress of 79 MPa. With regards to the deeper sea level (Fig. 20b), the responses show a great difference between leg members. The maximum responses are 77 MPa, and belong to leg 2 and leg 3 of the jacket.

6.2. Structural performances under design load cases (DLCs) + environmental loads (env)

The main objective is to identify the critical directionality under various loading conditions. With this aim, each selected jacket
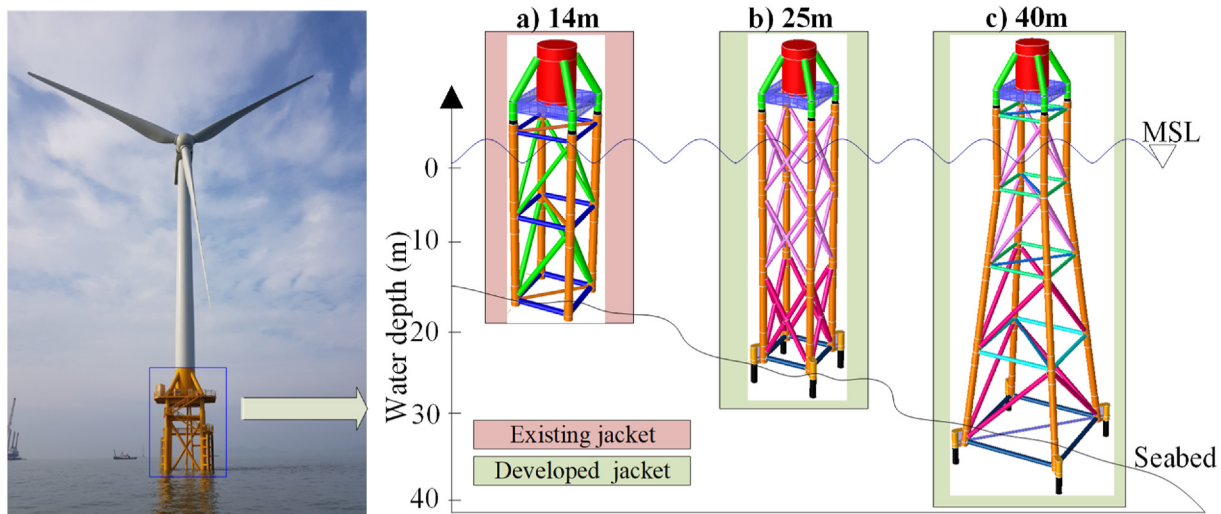

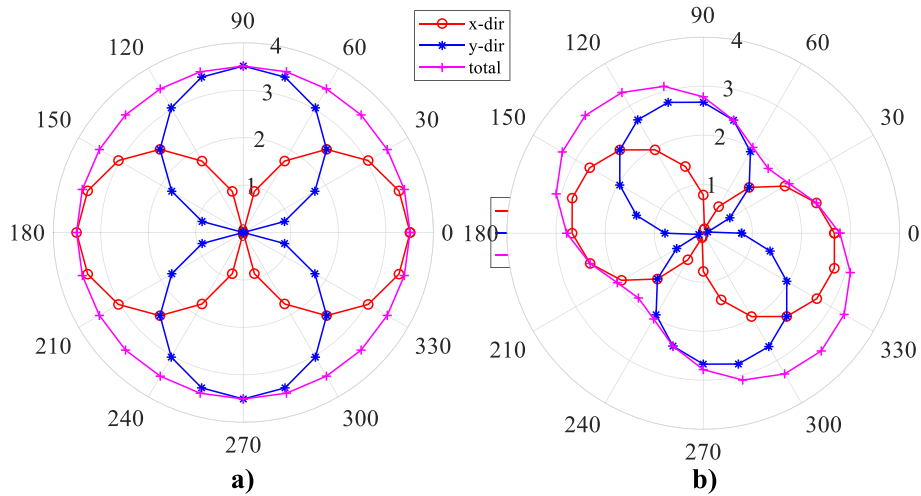**Fig. 17.** Suggested jacket substructures at different water depths.

Fig. 19. Polar diagrams of the lateral displacements: (a) 4LJ-25-1X and (b) 4LJ-40-2P [cm].
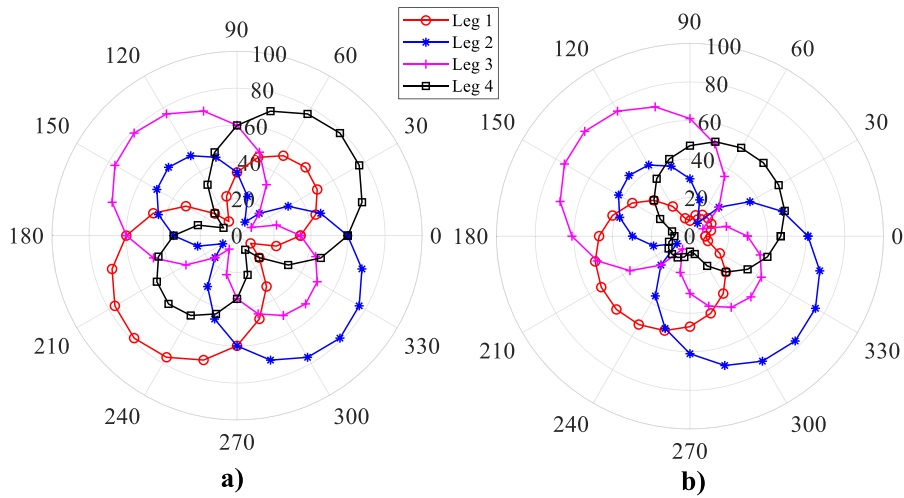

Fig. 20. Polar diagrams of the stresses: (a) 4LJ-25-1X and (b) 4LJ-40-2P [MPa].
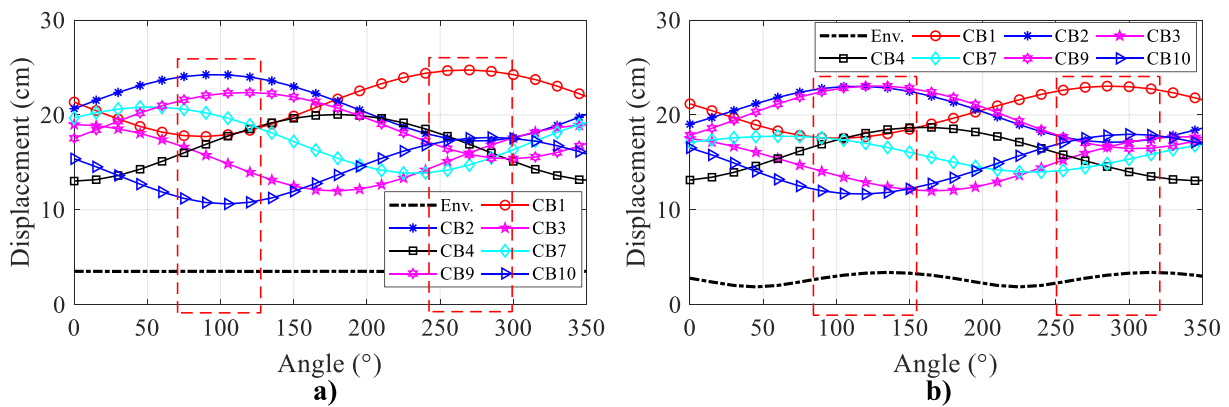

Fig. 21. Lateral displacement under combined loads: (a) 4LJ-25-1X and (b) 4LJ-40-2P [cm].

substructure was analyzed with a total of 288 analysis cases, comprising the various combinations of the environmental (24 cases) and design loads (12 cases) (see Fig. 18).

Fig. 21 illustrates the total displacements of the jacket structure against the combined loads (CBs). As explained in Section 5.2, structural responses are primarily caused by forces and moments in
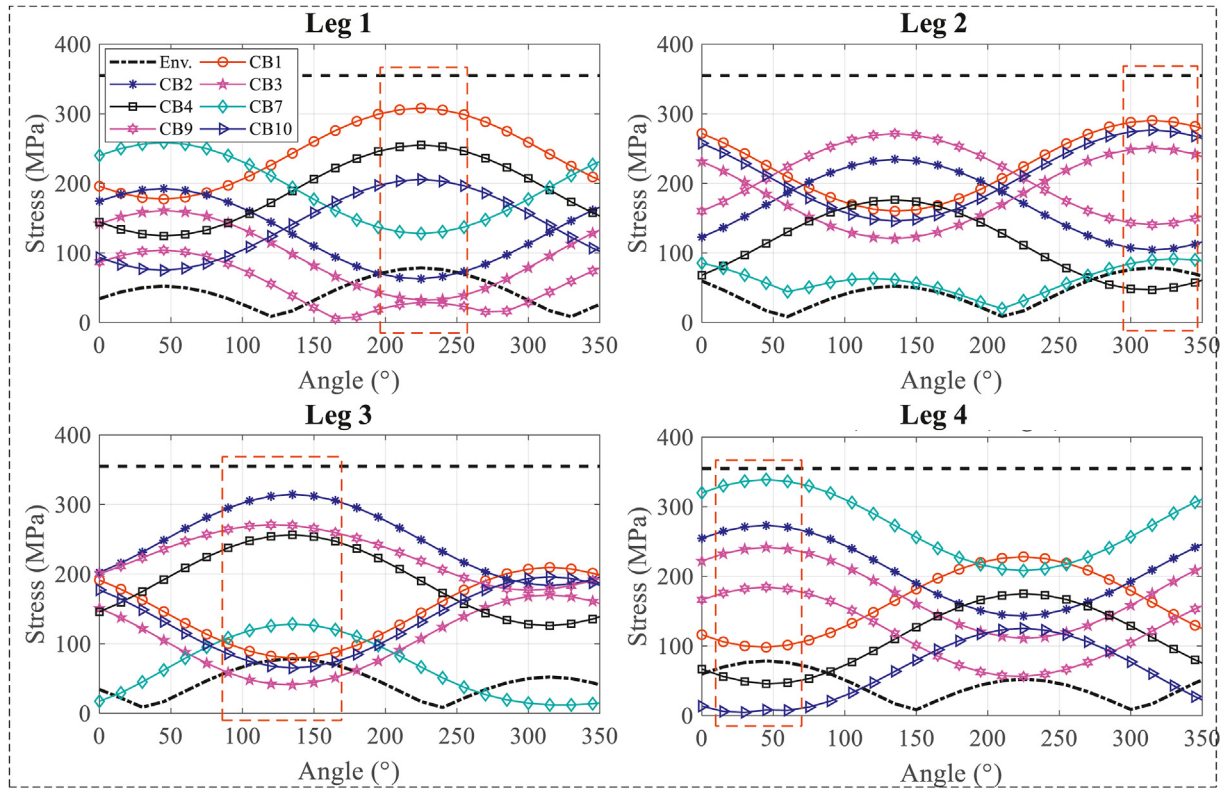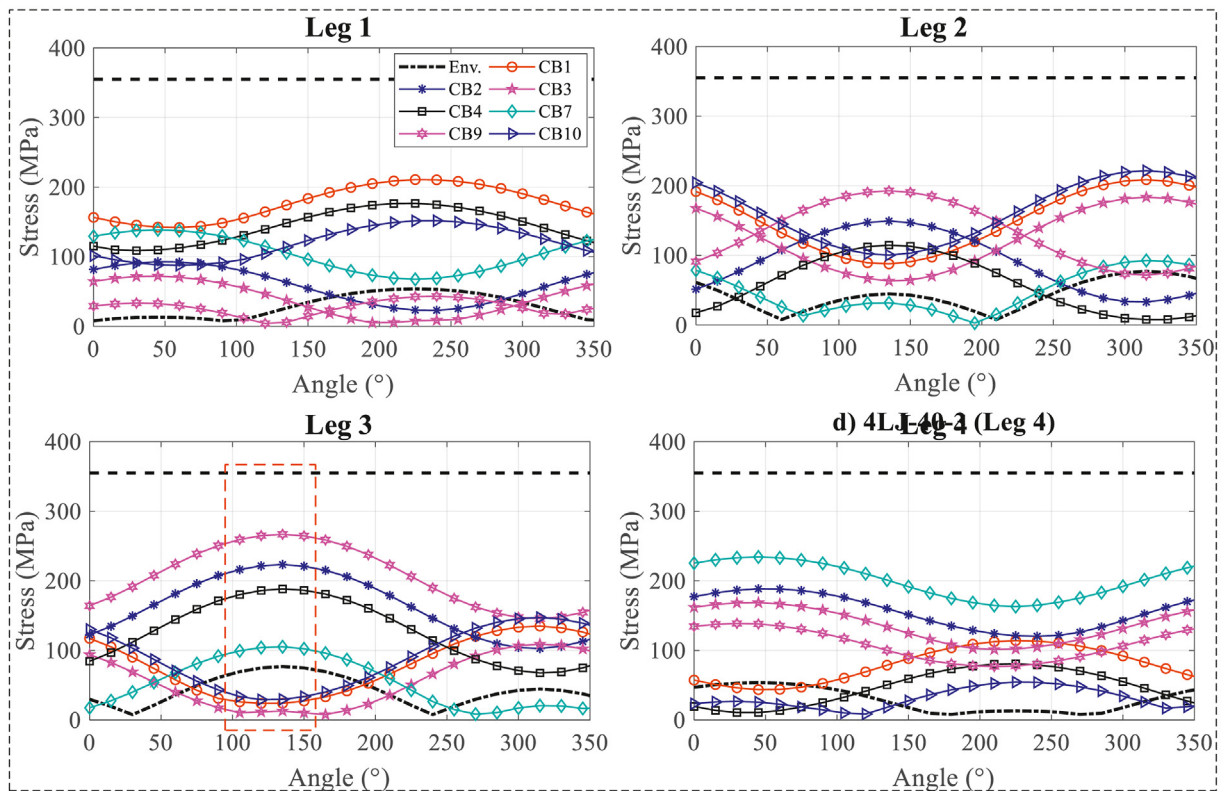
Fig. 22. Stresses under combined loads: (a) 4LJ-25-1X and (b) 4LJ-40-2P [MPa].

the X- and Y- directions. Thus, only seven CBs (i.e., CB1, CB2, CB3, CB4, CB7, CB9, CB10), which show larger responses compared to the other cases, are provided herein. The outcomes from the CBs are much larger compared to the environmental load (dash-dotted black line). At the water depth of 25 m (Fig. 21a), the maximum responses (24 cm) for CB1 and CB2 occur at the angles of 270 ° and 90 °, respectively. In the case of deeper water (Fig. 21b), the maximum displacements of the jacket substructure occur at the angles of 285 ° and 120 °. Based on the obtained outcomes, the critical regions (dash red rectangular) are defined. The angles in these ranges will cause the highest responses for the jacket substructure.

Like displacement, critical regions for stresses are also defined. This can be seen in Fig. 22, where the stress responses for each leg member are depicted. In general, under the CBs, the maximum stresses of all leg members are less than the yield strength of the material (355 MPa). In the cases of 4LJ-25-1X (Fig. 22a), the average stress is 313.0 MPa, and the highest stress occurs to leg 4 (339.1 MPa). As seen, the critical directions are different for each leg member due to influences of the design load cases. The critical responses of leg 1 and leg 2 are mainly caused by the CB1. On the other hand, the critical regions of leg 3 and leg 4 are mainly produced by CB2 and CB7, respectively. From the observation, the critical regions of the jacket substructure are defined and caused by the moments (CB1 and CB2) and forces (CB7) in the X-direction.

However, there is a distinct difference in the stress distribution of 4LJ-40-2P, as displayed in Fig. 22b. As shown, leg 3 is subjected to the largest stress (266.9 MPa), with a maximum difference of up to 21.1%, compared to other leg members. The critical bending directions are found to occur at angles varying between 105 ° and 150 ° under CB9, which is caused by the moment in the Y-direction.

7. Limitations

It is noted that the jacket substructures are developed in relation to the given wind turbine configuration and water depth. For a larger wind turbine, a classical similarity rule with the upscaling coefficients is recommended. The design approach for the larger wind turbines corresponds to the approach of the 3 MW reference wind turbine.

Even though this limitation, this study provides applicable knowledge of the design assessment of jacket substructures, which might be extended to the study of larger wind turbine cases. The feasible configuration should be examined the sensitivities of topological forms or bracing systems, and environmental loading directionality.

8. Conclusions

With the aim of developing offshore wind farms in deep water sites, this study conducted a feasibility analysis for jacket substructures at different water depths (i.e., 25 m and 40 m). For each sea level, four configurations with different topological

configurations and brace systems were discussed. To explore reasonable jacket substructures, this study considered jackets that fulfilled all main design requirements in terms of the target frequency and dynamic performances under ultimate loads. A comparison of structural weights is also reported. The results are summarized as follows:

- The topological configurations of jackets have a significant influence on the natural frequencies of the whole system, whereas the brace systems have small impacts on the dynamic characteristics of the jacket substructures. Thus, when designing a jacket substructure, the highest priority is to select an appropriate topological configuration.
- With regards to strength check, all jacket members and joints are within the safety zone. The high-stress distribution of the jacket substructure mainly occurs at the top layers due to the bending effect. Under ultimate loads, the Pratt type reaches its ultimate strength earlier than X-type.
- By comparing the effectiveness of different jacket substructures, two reasonable jacket substructures corresponding to different sea levels (i.e., 25 m and 40 m) are suggested. These jacket substructures will yield the best performance under Korean environmental conditions. Furthermore, they are feasible in terms of the availability of installing equipment for the Korean offshore wind farm.
- Furthermore, the critical bending directions of the selected jacket substructure are determined. At the water depth of 40 m, the critical bending directions vary between 105° and 150°, while the jacket substructure installed at 25 m is almost independent of the environmental loads.

The results of this study are significant, as they provide a framework for the development of jacket substructures with a representative turbine. Two reasonable jacket concepts are suggested and can be used as references for large-scale deployments in South Korea.
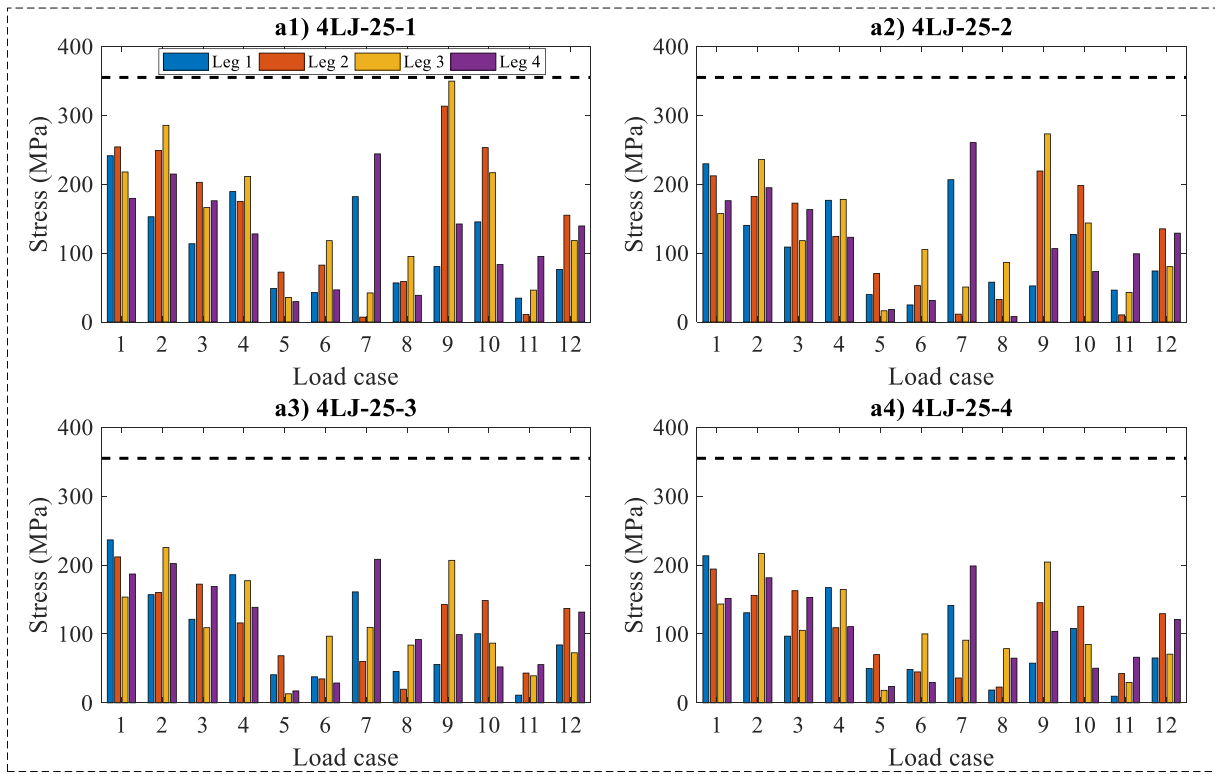
Declaration of competing interest

The authors declare that they have no known competing financial interests or personal relationships that could have appeared to influence the work reported in this paper.
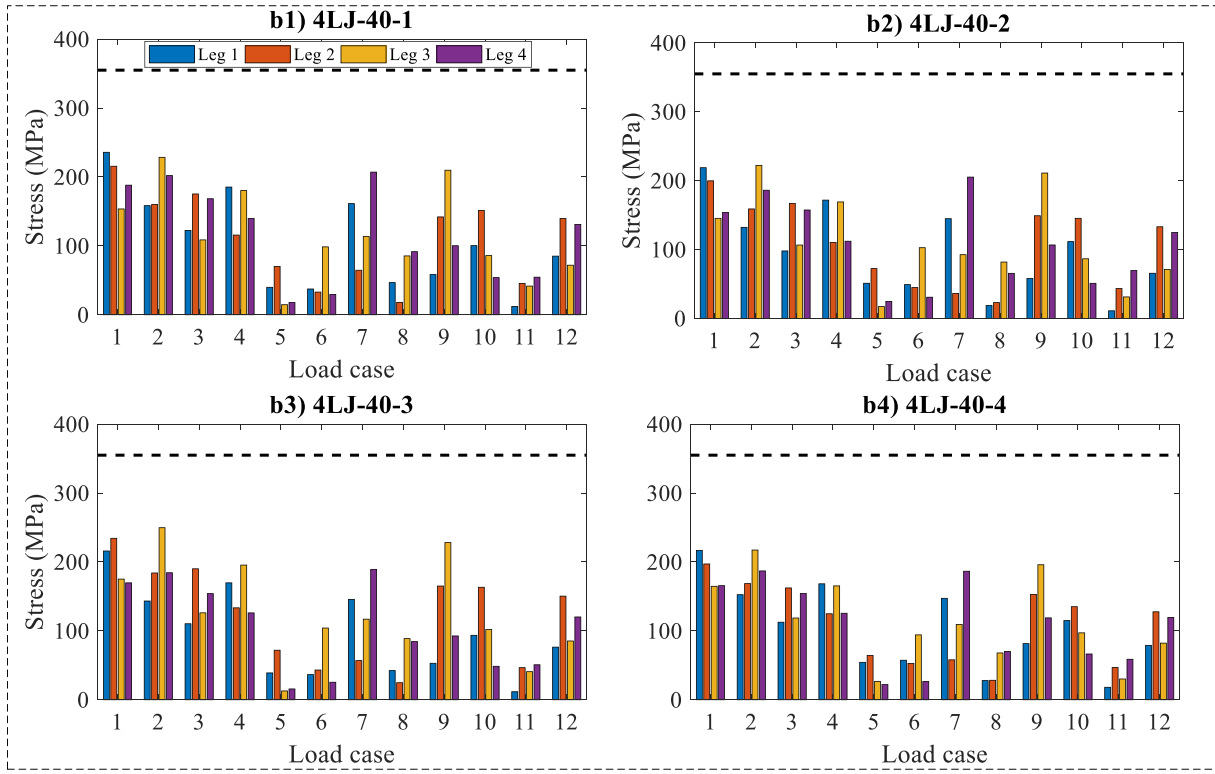
Acknowledgments

Appendix

a)

b)

Histograms of Stress: (a) 4LJ-25 and (b) 4LJ-40 [MPa].

References

4 C Offshore, 2021. Offshore Wind Farms in South Korea [WWW Document]. https://www.4coffshore.com/windfarms/south-korea/.

Bentley, 2019. Structural analysis computer system (SACS). User's Manual, Release 14 version 0, Engineering Dynamics.

Böker, C., 2010. Load Simulation and Local Dynamics of Support Structures for Offshore Wind Turbines. Shaker.

Bossanyi, E., 2010. GH-bladed Version 4.0 User Manual.

DNV-OS-J101, 2014. Design of Offshore Wind Turbine Structures.

DNVGL-ST-0126, 2018. Support Structures for Wind Turbines.

EEA, 2009. European Environment Agency. Europe's Onshore and Offshore Wind Energy Potential an Assessment of Environmental and Economic Constraints. https://doi.org/10.2800/11373.

El-Reedy, M.A., 2014. Marine Structural Design Calculations, Marine Structural Design Calculations. Elsevier Inc. https://doi.org/10.1016/C2012-0-07922-7.

IEC 61400-1, 2005. Wind Turbines-Part 1: Design Requirements.

IEC 61400-3, 2009. Wind Turbines - Part 3: Design Requirements for Offshore. Wind Turbines, Switzerland.

Jalbi, S., Bhattacharya, S., 2018. Closed form solution for the first natural frequency of offshore wind turbine jackets supported on multiple foundations incorporating soil-structure interaction. Soil Dynam. Earthq. Eng. 113, 593–613. https://doi.org/10.1016/j.soildyn.2018.06.011.

Jalbi, S., Bhattacharya, S., 2020. Concept design of jacket foundations for offshore wind turbines in 10 steps. Soil Dynam. Earthq. Eng. 139, 106357. https://doi.org/10.1016/j.soildyn.2020.106357.

Kang, K.-S., Lee, J.-S., Kim, J.-Y., Ryu, M.-S., 2011. Economic analysis of offshore wind farm considering domestic development conditions of Korea. Korea Wind Energy Jounal 2, 37–43.

Kim, D.H., Lee, S.G., 2015. Reliability analysis of offshore wind turbine support structures under extreme ocean environmental loads. Renew. Energy 79, 161–166. https://doi.org/10.1016/j.renene.2014.11.052.

Kim, D.H., Lee, S.G., Lee, I.K., 2014. Seismic fragility analysis of 5MW offshore wind turbine. Renew. Energy 65, 250–256. https://doi.org/10.1016/j.renene.2013.09.023.

Kim, S.Y., Kim, K.M., Park, J.C., Jeon, G.M., Chun, H.H., 2016. Numerical simulation of wave and current interaction with A fixed offshore substructure. Int. J. Nav. Archit. Ocean Eng. 8, 188–197. https://doi.org/10.1016/J.IJNAOE.2016.02.002.

Kim, J.H., Kim, S.Y., Yoo, S.H., 2020. Public acceptance of the "renewable energy 3020 plan": evidence from A contingent valuation study in South Korea. Sustain. Times 12. https://doi.org/10.3390/SU12083151.

NORSOK, 2004. Standard Design of Steel Structure. DNV.

Oh, K.Y., Nam, W., Ryu, M.S., Kim, J.Y., Epureanu, B.I., 2018. A review of foundations of offshore wind energy convertors: current status and future perspectives. Renew. Sustain. Energy Rev. https://doi.org/10.1016/j.rser.2018.02.005.

POSCO, 2017. 4-Leg Jacket Substructure for 3MW Offshore Wind Turbine, Structural Design Report.

Sandal, K., Latini, C., Zania, V., Stolpe, M., 2018. Integrated optimal design of jackets and foundations. Mar. Struct. 61, 398–418. https://doi.org/10.1016/J.MARSTRUC.2018.06.012.

Shi, W., Park, H., Chung, C., Baek, J., Kim, Y., Kim, C., 2013a. Load analysis and comparison of different jacket foundations. Renew. Energy 54, 201–210. https://doi.org/10.1016/j.renene.2012.08.008.

Shi, W., Park, H., Han, J., Na, S., Kim, C., 2013b. A study on the effect of different modeling parameters on the dynamic response of A jacket-type offshore wind turbine in the Korean southwest sea. Renew. Energy 58, 50–59. https://doi.org/10.1016/j.renene.2013.03.010.

Shi, W., Han, J., Kim, C., Lee, D., Shin, H., Park, H., 2015. Feasibility study of offshore wind turbine substructures for southwest offshore wind farm project in Korea. Renew. Energy 74, 406–413. https://doi.org/10.1016/j.renene.2014.08.039.

Tran, T.-T., Hussan, M., Kim, D., Nguyen, P.-C., 2020. Distributed plasticity approach for the nonlinear structural assessment of offshore wind turbine. Int. J. Nav. Archit. Ocean Eng. 12, 743–754.

Tran, T.-T., Kang, S., Lee, J.-H., Lee, D., 2021. Directional bending performance of 4-leg jacket substructure supporting a 3MW offshore wind turbine, 2021 Energies 14, 2725. https://doi.org/10.3390/EN14092725. Page 2725 14.

Tran, T.T., Kim, E., Lee, D., 2022. Development of a 3-legged jacket substructure for installation in the southwest offshore wind farm in South Korea. Ocean Eng. 246, 110643. https://doi.org/10.1016/J.OCEANENG.2022.110643.

Wu, X., Hu, Y., Li, Y., Yang, J., Duan, L., Wang, T., Adcock, T., Jiang, Z., Gao, Z., Lin, Z., Borthwick, A., Liao, S., 2019. Foundations of offshore wind turbines: a review. Renew. Sustain. Energy Rev. 104, 379–393.